Available online at www.sciencedirect.com
SCIENCE DIRECT®
Journal of Power Sources 135 (2004) 72–78
JOURNAL OF POWER SOURCES
www.elsevier.com/locate/jpowsour

Novel infiltrated Phlogopite mica compressive seals for solid oxide fuel cells

Yeong-Shyung Chou*, Jeffry W. Stevenson

Material Science Division, Pacific Northwest National Laboratory, P.O. Box 999, Richland, WA 99352, USA

Received 23 January 2004; accepted 21 February 2004

Available online 8 July 2004

Abstract

A novel compressive Phlogopite mica seal was developed that showed superior thermal cycle stability with very low leak rates at 800 °C. A commercially available Phlogopite mica paper was infiltrated with a wetting or melt-forming agent, and tested in a hybrid form during thermal cycling. The results of H_3BO_3-infiltrated mica showed a continued decrease in leak rates over thermal cycling, and very low rates ($<5 \times 10^{-4}$ sccm/cm) were obtained after ~15 thermal cycles. The results of Bi-nitrate infiltrated mica exhibited a constant leak rate of $(1–4) \times 10^{-3}$ sccm/cm over 36 thermal cycles. The leak rates of the infiltrated mica were one to two orders of magnitude lower than leak rates for the as-received micas. Open circuit voltage tests were also conducted using dense 8YSZ plates to assess the effectiveness of the mica seals. Open circuit voltages equivalent to, or close to, the theoretical (Nernst) values were obtained.

Keywords: Thermal cycling; Compressive seal; Phlogopite mica; Leak rate; Open circuit voltage

1. Introduction

One of the critical challenges facing planar solid oxide fuel cell (SOFC) developers is the need for reliable sealing technology. Seals are required which will offer long-term stability in the high temperature SOFC environment and also maintain their integrity during thermal cycling. Currently, there are three primary approaches for SOFC seal development: glass (or glass-ceramics) seals [1–4], metallic brazes [5,6], and compressive seals [7–11]. The use of compressive seals offers a unique advantage over the other approaches in that a stringent matching of the coefficient of thermal expansion (CTE) of the various SOFC stack components is not necessary. Currently, the development of compressive seals is primarily focused on mica-based seals. Chou et al. recently developed novel hybrid mica seals through which the 800 °C leak rates were reduced two to three orders of magnitude by adding a glass or metal interlayer between the mica materials and adjacent stack components [7,8]. These Muscovite mica-based seals also showed good thermal stability when held for about 500 h in air or reducing environments at elevated temperatures [10]. The cleaved Muscovite mica sheets, however, suffered a rapid increase in leak rate during thermal cycling, due to wear damage from the repeated cycles; in some cases, the leak rates tended to stabilize after 20–30 thermal cycles [11]. The objective of the present study is to develop a compressive mica seal offering constant, low leak rates during repeated thermal cycling. In this paper, we present a novel sealing approach based on commercially available Phlogopite mica papers infiltrated with forming materials. Results of leak rate and open circuit voltage (OCV) testing of these infiltrated mica seals are reported and compared with results for glass-ceramic seals.

2. Experimental

2.1. Materials

The mica used in this study is a commercially available Phlogopite mica paper (McMaster-Carr, Atlanta, GA). The mica paper is composed of compressed discrete mica flakes (Fig. 1A). Due to the anisotropic morphology of the mica flakes, they are highly oriented, with their basal planes (cleavage plane) overlapping with each other (Fig. 1B). Two Phlogopite mica papers were used in this study. One is about 0.004 in. thick and contains 3–5% of organic binders (mica-A). The other is about 0.003 in. thick and

* Corresponding author. Tel.: +1-509-375-2527; fax: +1-509-375-2186.
E-mail address: yeong-shyung.chou@pnl.gov (Y.-S. Chou).

0378-7753/$ – see front matter © 2004 Published by Elsevier B.V.
doi:10.1016/j.jpowsour.2004.02.037

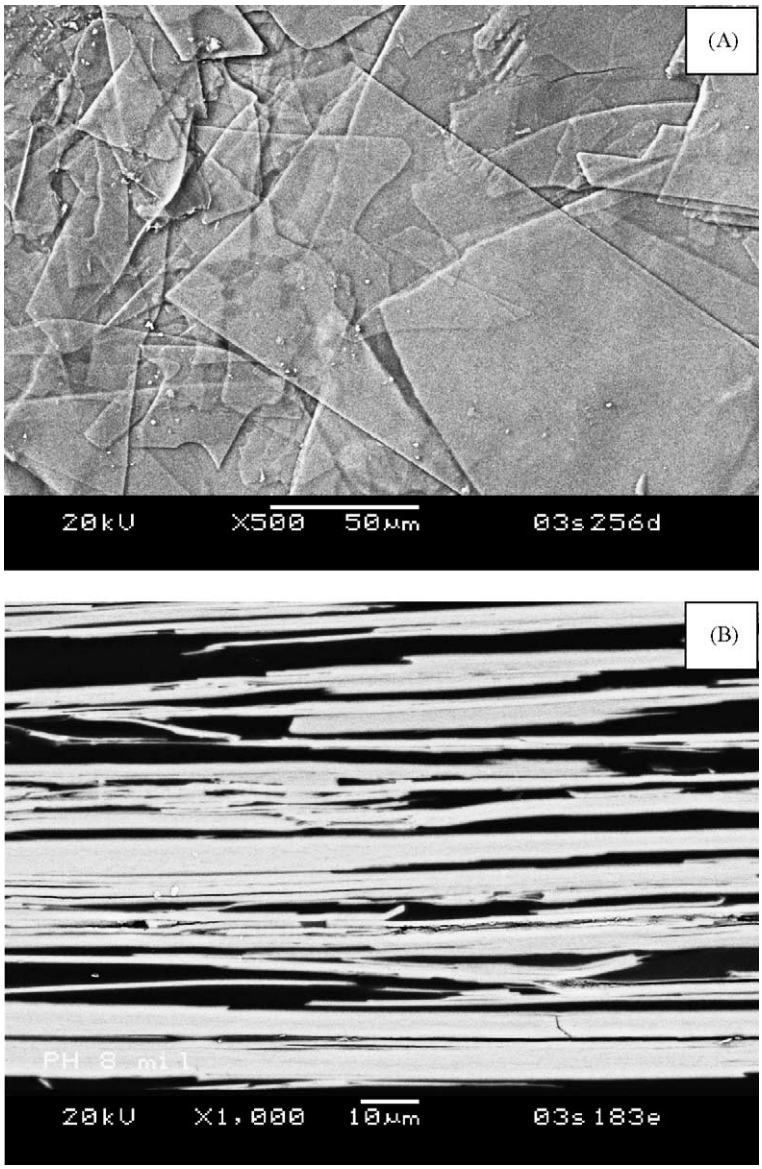

Fig. 1. Morphology and microstructure of the Phlogopite mica paper: (A) top surface and (B) cross-section.

contains no binders (mica-B). Both materials have similar color and surface textures. Prior to infiltration, mica-A was first heat-treated at 700 °C for 4 h to remove the binders. Mica-B was used as-received. For the infiltration, two chemicals were used: H_3BO_3 (99.5% Alfa Aesar, MA) and $Bi(NO_3)_3{\cdot}5H_2O$ (98%, Alfa Aesar, MA). De-ionized water was used to make saturated H_3BO_3 or Bi-nitrate solutions. Due to low room temperature solubility, the concentration of the boric acid solution was increased by adding additional H_3BO_3 and heating to 70–90 °C with a solubility about 17–30 g/100 g H_2O. Mica-A discs (about 1.5 in. in diameter) were immersed into the saturated H_3BO_3 solution for a couple of minutes, removed, and dried at ∼50 °C. Bi-nitrate solutions were also made in a similar manner and the infiltration was conducted on mica-B with pipette instead of immersing the mica discs into the solutions.

2.2. Leak test, thermal cycling, and mid-term stability test

Leak rate tests of the infiltrated mica discs were conducted by pressing them between an Inconel 600 pipe and an alumina substrate or a metal plate. A compressive stress of 100 psi was maintained throughout the whole test, including the heating and cooling cycles. The leak rates were determined with high-purity helium at a gauge pressure of 2 psi. Thermal cycling was conducted between 100 and 800 °C. A mid-term thermal stability test was also carried out on the Bi-nitrate infiltrated mica. The infiltrated mica was held at 800 °C for 250–500 h in either air or a humid reducing (2.71% H_2/Ar+ ∼ 3% H_2O) environment, and leak rates were measured as a function of the time. Details of the leak test, leak rate determination, the temperature profiles

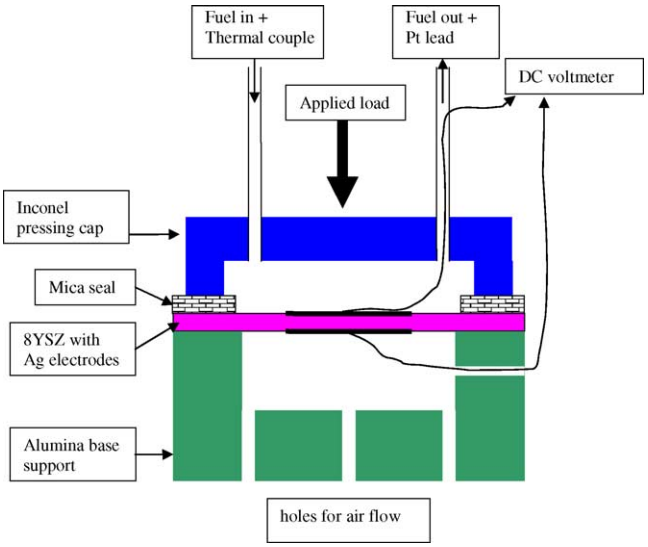

Fig. 2. Schematic showing the test fixture for open circuit voltage test of dense 8YSZ plate with compressive mica seals.

for thermal cycling, and mid-term stability test are given in [7,10,11].

2.3. Open circuit voltage test

In order to assess the sealing capability of the mica seals, open circuit voltage tests were conducted on 8YSZ electrolyte plates with various mica seals. 2 in. × 2 in. dense 8YSZ plates were prepared by slip casting fine 8YSZ powders (TOSOH, Zirconia, TZ-8Y, Japan), followed by sintering at 1450 °C for 2 h. The sintered plates were machined to the desired size and thickness (~1–2 mm), and then screen printed with silver paste electrodes on both sides. After electrode firing, Pt wire leads were connected for the OCV tests. The dense 8YSZ plate was then pressed between an Inconel pressing cap and an alumina base support. The infiltrated micas were placed between the 8YSZ and the Inconel fixture. A schematic drawing of the OCV test fixture is shown in Fig. 2. The OCV measurements were conducted at 800 °C after dwelling at the temperature for about 2 h. A low-hydrogen content fuel (2.71% H_2/Ar+ ~ 3% H_2O) was used on the anode side (with variable flow rates) and air was used as the oxidant on the cathode side.

3. Results and discussion

3.1. Concept of "infiltrated" micas

In earlier work, it was found that the major leak paths for compressive mica seals were at the interfaces between the mica and the adjacent materials being sealed (metal or ceramics). These leak rates of the monolithic Muscovite micas can be substantially reduced (two to three orders of magnitude) by adding extra compliant layers (glass or metal foil) at these interfaces to form the so-called "hybrid mica seals" [7,8]. However, the leak rates in these seals increased rapidly during initial thermal cycles. Further testing on Phlogopite mica papers (in hybrid form) showed different behaviors of leak rate versus thermal cycling that the leak rates gradually decreased with increasing of thermal cycles [12]. From microstructural observation, it was found that some of the glass (from the compliant layers) penetrated into the mica papers and resulted in leak rates insensitive to thermal cycles. Microstructural examination of the mica papers verified the presence of voids between the discrete mica flakes (Fig. 1B) which form continuous 3D leak paths through the paper. In the present study, infiltration of a wetting or glass forming material into the mica papers was investigated as a potential means of interrupting the continuous 3D leak paths to 2D geometry, thereby reducing the leak rate through the material. It is expected that the more flat the fracture surfaces (leak paths), the more close geometrical match when they are compressed against each other. This would result in narrower gap between the fracture planes, and lead to lower leak rates and less damages upon thermal cycling. The concept of the "infiltrated" micas is illustrated in Fig. 3 where the infiltrated materials will wet or necking at the voids and form a controlled 2D leak path upon thermal cycles (dotted line in Fig. 3).

3.2. Selection of chemicals for infiltration

To evaluate the "infiltrated" mica concept, two chemicals were selected as infiltrants: boric acid (H_3BO_3) and bismuth nitrate ($Bi(NO_3)_3{\cdot}5H_2O$). Boric acid converts to B_2O_3 upon heating and was expected to form a wetting liquid at elevated temperatures (the mp of B_2O_3 is ~450 °C). Similarly, bismuth nitrate converts to Bi_2O_3 in air. Bismuth oxide has a higher mp (~813 °C), but was expected to be very compliant at 800 °C, leading to the possibility that it could be squeezed into the voids between flakes when compressive stresses were applied. It needs to be noted that these two chemicals may not offer satisfactory long-term stability in SOFC operating environments. However, they were consid-

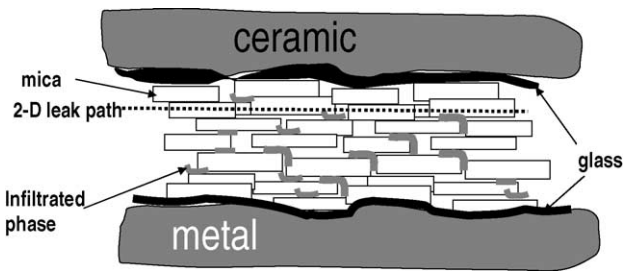

Fig. 3. Schematic showing the concept of infiltrated mica in which the continuous voids between discrete mica flakes (Fig. 1B) are filled or blocked with an infiltrated wetting or compliant phase such that upon thermal cycling a desirable 2D leak path (dotted line) will form instead of a 3D path.

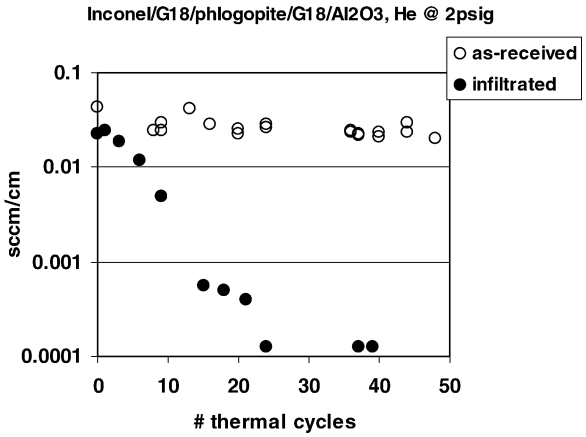

Fig. 4. Effect of thermal cycling on the 800 °C normalized leak rates of the Phlogopite mica in the as-received and the H_3BO_3-infiltrated forms. The mica was pressed between an Inconel pipe and an alumina substrate at 100 psi in air.

ered to be appropriate choices for these proof-of-concept experiments.

3.3. Thermal cycling of H_3BO_3-infiltrated Phlogopite micas

The results of the 800 °C thermal cycle leak rate tests of the H_3BO_3-infiltrated Phlogopite micas (in hybrid form, i.e., an extra glass (Ba–Al–silicate) layer was inserted above and below the infiltrated mica) are shown in Fig. 4. Previous results for the same mica without infiltration (also in hybrid form under the same compressive stress) are also included [12]. It is interesting to note that the leak rates of the infiltrated mica decreased abruptly with an increasing number of thermal cycles. The leak rates were $\sim 2.3 \times 10^{-2}$ sccm/cm initially, $\sim 5.5 \times 10^{-4}$ sccm/cm after 15 thermal cycles, and $\sim 1.3 \times 10^{-4}$ sccm/cm after 23 cycles. The reduction of leak rate is about two orders of magnitude. For the as-received mica, the leak rate was $\sim 4.3 \times 10^{-2}$ sccm/cm initially, and remained fairly constant (within the range of $(2.1–3.0) \times 10^{-2}$ sccm/cm) during the following 48 thermal cycles. It is evident that the presence of the B_2O_3 must have substantially blocked the leak paths between the mica flakes. It is not clear why the leak rates of the infiltrated micas were higher in the beginning than they were after ~23 thermal cycles. One possible cause is that the initial distribution of B_2O_3 was not uniform within the mica paper, but instead was more highly concentrated on the outer surfaces of the mica samples. During the test period, B_2O_3 may have gradually penetrated into the mica paper, steadily blocking the continuous leak paths between discrete mica flakes. Post-test observation showed that the mica sample could be easily detached from the Inconel test fixtures, indicating that the B_2O_3 did not react with the mica (an alumina silicate mineral) to form a significant amount of glass at the interface.

3.4. Thermal cycling of Bi-nitrate infiltrated Phlogopite micas

The leak tests of the Bi-nitrate infiltrated micas were conducted in a different way from the previous H_3BO_3-infiltrated mica tests. To examine the effect of mismatch in coefficient of thermal expansion, the Bi-nitrate infiltrated micas were tested in three different metal–metal couples. The infiltrated micas were pressed between an Inconel 600 pipe and one of three different metal support plates: Inconel 600, Haynes 230, and SS430. The average CTE (RT to 800 °C) of Inconel 600, Haynes 230, and SS430 are ~17, ~15, and ~12.5 ppm/°C, respectively. The CTE of the Phlogopite mica (along the basal plane) is ~11 ppm/°C. Inconel 600 and Haynes 230 are superalloys with superior thermal and mechanical properties. However, due to their very high CTEs, they can only be considered as SOFC interconnect candidates if compliant seals (such as compressive seals) are used. SS430 has a good CTE match with typical anode-supported SOFCs, but suffers severe oxidation at 800 °C. Our tests of the infiltrated mica in these three metal couples therefore covered a wide range of CTE mismatch over which other sealing approaches (e.g., glass seals and brazes) are not likely to be suitable.

The leak rates versus thermal cycling of the infiltrated mica in the three metal couples are shown in Fig. 5. It is interesting to note that the leak rates are much lower for all three metal couples, i.e., less than 4×10^{-3} sccm/cm, than for the as-received mica ($(2.1–4.3) \times 10^{-2}$ sccm/cm in Fig. 4). Leak rates through the Bi-nitrate infiltrated mica appeared to be independent of the wide range of CTE mismatches among the three metal couples. In addition, the leak rates were rather insensitive to the number of thermal cycles (the fluctuation of leak rates during the 36 cycles is likely due to ambient temperature fluctuations). Compared to the H_3BO_3-infiltrated micas, the Bi-nitrate infiltrated micas showed low leak rates in the first cycle instead of a grad-

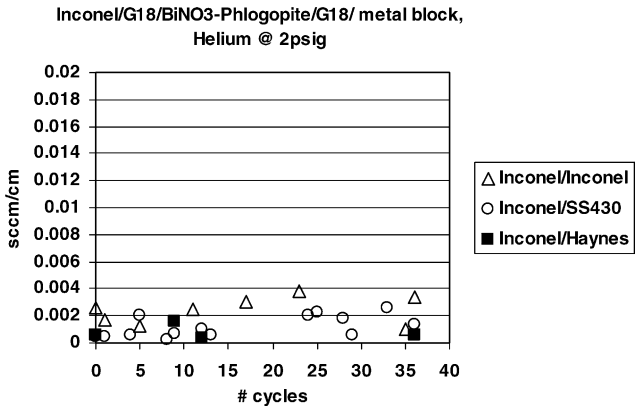

Fig. 5. Effect of thermal cycling on the 800 °C normalized leak rates of the Bi-nitrate infiltrated Phlogopite micas. The infiltrated micas were pressed between three metal couples: Inconel 600/Inconel 600, Inconel 600/Haynes 230, and Inconel 600/SS430 at 100 psi in air.

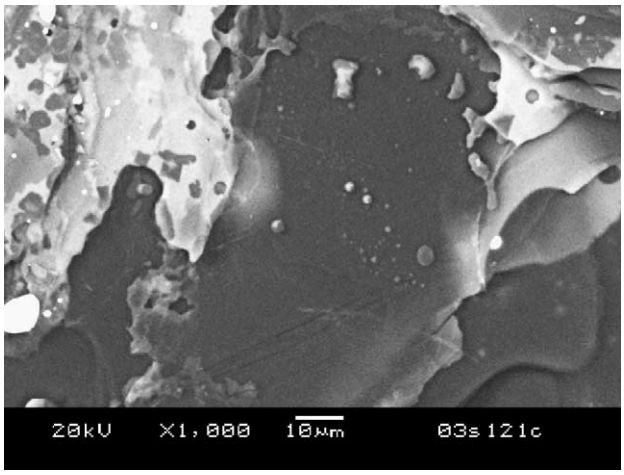

Fig. 6. Scanning electron micrograph showing the fracture surface of the Bi-nitrate infiltrated mica after 37 thermal cycles in air at 100 psi. The white phase is Bi_2O_3 and the gray phase is mica.

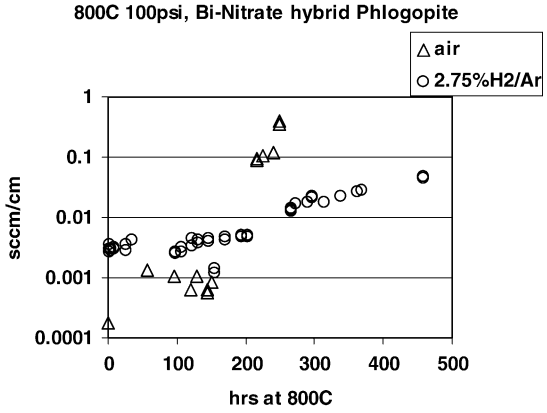

Fig. 7. Thermal stability test of the Bi-nitrate infiltrated Phlogopite mica in air and in a reducing (2.71% H_2/Ar+ ∼ 3% H_2O) environment at 800 °C. The mica was pressed between an SS430 loading pipe and an SS430 substrate (0.02 in. thick).

ual decrease with thermal cycles. This behavior is likely due to the presence of excess Bi-nitrate on the mica surfaces as well as the thinner mica used (mica-B). It was found that bismuth nitrate ($Bi(NO_3)_3{\cdot}5H_2O$) did not form a stable aqueous solution but decomposed to form $BiONO_3{\cdot}H_2O$ white precipitates. After infiltration and drying, a coating of the precipitate remained on the mica discs. In post-cycling microstructural characterization, it was also found that the mica could be easily detached from the test fixtures. The penetration of Bi_2O_3 into the mica paper (the white phase in Fig. 6) and the smooth fracture surface of the cleaved mica (gray phase) were evident during scanning electron microscopy.

3.5. Thermal stability test of Bi-nitrate infiltrated Phlogopite micas

The Bi-infiltrated Phlogopite micas were also subjected to thermal stability tests at constant temperature (800 °C) in two environments: air and 2.71% H_2/Ar+ ∼ 3% H_2O. The mica discs were pressed between an SS430 loading pipe and an SS430 substrate (0.02 in. thick). Results of the tests are plotted in Fig. 7. The infiltrated mica tested in air showed a sharp increase in leak rates from about 0.001 to about 0.1 sccm/cm after ∼150 h. Post-test observation found that the 0.02 in. thick SS430 substrate suffered severe oxidation and corrosion by molten Bi_2O_3, causing the SS430 substrate to become brittle and cracked, which resulted in the rapid increase in leak rate. For the infiltrated mica tested in the reducing environment, the leak rates were fairly constant during the first ∼200 h, but appeared to increase linearly with time afterwards. The cause of the gradual increase in leak rate was apparently the volatilization of Bi_2O_3 in the reducing environment at elevated temperatures; the loss of Bi_2O_3 gradually opened up leak paths through the mica paper. Clearly, Bi_2O_3 is not suitable for long-term application in SOFC environments; evaluations of other alternative "infiltrants" such as glass or glass-ceramics are in progress and will be reported in the near future.

3.6. Open circuit voltage tests

In addition to the quantitative leak rate measurements described above, open circuit voltage tests were also performed. OCV measurements provide information regarding the effectiveness of the seal by allowing a comparison of the observed cell voltage at open circuit with the theoretical voltage which should be obtained if there is no mixing or dilution of the oxidant and fuel gases. (If the cell is completely sealed, the OCV should correspond to the value calculated by the Nernst equation.) The OCV tests thus provide a useful complement to the leak rate measurements, especially since the maximum acceptable leak rates for SOFC stacks have not yet been defined and are likely to be design-specific.

Open circuit voltage tests were conducted on Bi-nitrate infiltrated micas, and, for comparison, on a glass seal and on plain Phlogopite mica (without infiltration and not in the hybrid form). For the OCV tests, only the fuel side was sealed and a low-hydrogen fuel (2.71% H_2/Ar with ∼3% H_2O) was used. Although actual fuels for SOFC operation are much higher in hydrogen content, the use of 2.71% H_2/Ar fuel offered advantages of higher safety and better sensitivity of leaks from the air side into the fuel side. The results of the OCV tests at various fuel flow rates are plotted in Fig. 8. The Nernst voltage of the fuel gas, i.e., 2.71% H_2/Ar with ∼3% H_2O versus air at 800 °C, was calculated to be 0.934 V. It is evident that the OCVs of the glass seal and the Bi-infiltrated micas were in agreement with the theoretical voltages (within ±0.5%) indicating the sealing capability of the infiltrated mica was as good as the sealing glass (at least for this OCV test). In addition, the effect of the fuel flow rate appeared to be very minute as the OCV only changed by a few millivolts when the flow rate was increased from 25 to about 200 sccm.

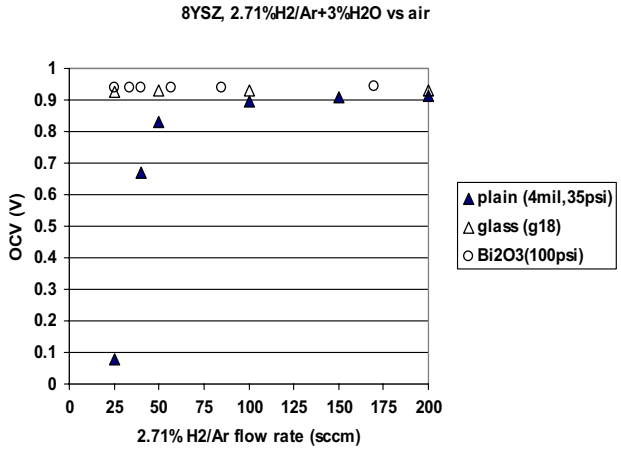

Fig. 8. Open circuit voltage tests of 2 in. × 2 in. dense 8YSZ electrolyte plates with various seals at different fuel flow rates: glass seal (open triangle), plain mica (filled triangle), and Bi-nitrate infiltrated mica (circle). 2.71% H_2/Ar (with ∼3% H_2O) was used as fuel against air and the Nernst voltage was calculated to be 0.934 V at 800 °C.

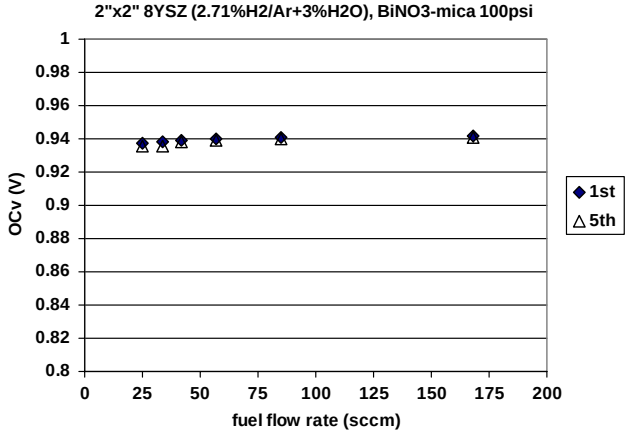

Fig. 9. Effect of thermal cycling on the open circuit voltage of 2 in. × 2 in. dense 8YSZ electrolyte plate with Bi-nitrate infiltrated mica as the compressive seal.

On the other hand, the plain mica showed OCVs much lower than the Nernst voltage (the plain mica was pressed at a much lower stress of 35 psi (this sample used a commercial 8YSZ thin electrolyte (∼200 μm thick) and could not take higher stresses without fracture), and was expected to have appreciable leak rates due to the leak paths within the material and at the interfaces between the mica and the adjacent materials, since glass interlayers were not used). In addition, the OCVs of the plain mica increased with increasing fuel flow rate. This suggests that the leak path of the current test fixture (Fig. 2) is from air into the fuel side; as the fuel flow rate increases, the air leak into the fuel has a diminishing diluting effect on the fuel gas composition (the air leak is expected to be relative constant since the pressure difference across the mica seal from the fuel side to air side is very minute). We have also changed the air flow rates on the air side and found no distinct changes in measured OCVs, implying that leak path from fuel side to air side is minimal. The current leak direction, i.e., air into fuel, is likely due to the faster flow of fuel inside the small test chamber compared to the slow flowing or stagnant surrounding air in the larger furnace chamber.

3.7. Open circuit voltage tests during short thermal cycling with infiltrated micas

The Bi-nitrate infiltrated Phlogopite mica was also subjected to several thermal cycles during OCV tests. The results were shown in Fig. 9. Over five thermal cycles, there was no significant change in the OCV, which remained close or equal to the Nernst voltage. In addition, no dependence of OCV on fuel flow rate was observed, consistent with good seal behavior. The sample, however, lost electrical contact after five thermal cycles. Post-test characterization showed extensive corrosion of a Pt wire lead by the Bi_2O_3, which had caused the wire to break. Although, as mentioned above, neither Bi_2O_3 or B_2O_3 are likely to be suitable infiltrants for long-term SOFC seal applications, the "infiltrated" Phlogopite micas were shown to offer low leak rates good thermal cycle stability, and OCVs similar to those for hermetic glass seals.

4. Conclusions

A novel compressive Phlogopite mica seal was developed that showed superior thermal cycle stability with very low leak rates at 800 °C. The "infiltrated" mica paper seal was demonstrated using commercial Phlogopite mica paper and a wetting or melt-forming agent (H_3BO_3 and bismuth nitrate). The results for H_3BO_3-infiltrated mica showed a continued decrease in leak rates over thermal cycling, and very low rates ($<5\times10^{-4}$ sccm/cm) were obtained after ∼15 thermal cycles. The results for Bi-nitrate infiltrated mica exhibited constant leak rates of $(1–4)\times10^{-3}$ sccm/cm over 36 thermal cycles and showed no dependence on CTE mismatches. The leak rates for the infiltrated mica were one to two orders of magnitude lower than for the as-received micas. Mid-term stability test at 800 °C showed that Bi_2O_3 was not suitable for long-term operation. Open circuit voltage tests were also conducted on 2 in. × 2 in. 8YSZ plates to assess the effectiveness of the mica seals. The results showed that OCVs equal or close to the Nernst voltage were obtained. The current results clearly demonstrate the viability of the concept of "infiltrated" micas as candidates for compressive seals for solid oxide fuel cells.

Acknowledgements

The authors would like to thank S. Carlson for SEM sample preparation, and J. Coleman for SEM analysis. This

paper was funded as part of the Solid-state Energy Conversion Alliance (SECA) Core Technology Program by the US Department of Energy's National Energy Technology Laboratory (NETL). Pacific Northwest National Laboratory is operated by Battelle Memorial Institute for the US Department of Energy under Contract no. DE-AC06-76RLO 1830.

References

[1] T. Yamamoto, H. Itoh, M. Mori, N. Mori, T. Watanabe, Compatibility of mica glass-ceramics as gas-sealing materials for SOFC, Denki Kagaku 64 (6) (1996) 575–581.
[2] K. Ley, M. Krumpelt, J. Meiser, I. Bloom, J. Mater. Res. 11 (1996) 1489.
[3] P. Larsen, C. Bagger, M. Morgensen, J. Larsen, in: M. Dokiya, O. Yamamoto, H. Tagawa, S. Singhal (Eds.), Solid Oxide Fuel Cells-IV, vol. 69, Electrochemical Society, Pennington, NJ, 1995, p. PV 95-1.
[4] N. Lahl, D. Bahadur, K. Singh, L. Singheiser, K. Hilpert, J. Electrochem. Soc. 149 (5) (2002) A607–A614.
[5] K.S. Weil, J.S. Hardy, J.Y. Kim, Use of a novel ceramic-to-metal braze for joining in high temperature electrochemical devices, in: Joining of Advanced and Specialty Materials V, American Society of Metals, 2002.
[6] K.S. Weil, J.S. Hardy, J.Y. Kim, Development of a silver-copper oxide braze for joining metallic and ceramic components in electrochemical devices, in: Proceedings of the International Brazing and Soldering 2003 Conference, American Welding Society, 2003.
[7] Y.-S. Chou, J.W. Stevenson, L.A. Chick, Ultra-low leak rate of hybrid compressive mica seals for solid oxide fuel cells, J. Power Sources 112 (1) (2002) 130–136.
[8] Y.S. Chou, J.W. Stevenson, L.A. Chick, Novel compressive mica seals with metallic interlayers for solid oxide fuel cell applications, J. Am. Ceram. Soc. 86 (6) (2003) 1003–1007.
[9] S.P. Simner, J.W. Stevenson, Compressive mica seals for SOFC applications, J. Power Sources 102 (2) (2001) 310–316.
[10] Y.S. Chou, J.W. Stevenson, Mid-term stability of novel mica-based compressive seals for solid oxide fuel cells, J. Power Sources 115 (2) (2003) 274–278.
[11] Y.S. Chou, J.W. Stevenson, Thermal cycling and degradation mechanisms of compressive mica-based seals for solid oxide fuel cells, J. Power Sources 112 (2) (2002) 376–383.
[12] Y.S. Chou, J.W. Stevenson, Phlogopite mica-based compressive seals for solid oxide fuel cells: effect of mica thickness, J. Power Sources 124 (2) (2002) 473–478.